AIChE WILEY InterScience DISCOVER SOMETHING GREAT

Filtration Model for Suspensions that Form Filter Cakes with Creep Behavior

Morten Lykkegaard Christensen and Kristian Keiding
Dept. of Biotechnology, Chemistry and Environmental Engineering, Aalborg University, 9000 Aalborg, Denmark

DOI 10.1002/aic.11108
Published online January 29, 2007 in Wiley InterScience (www.interscience.wiley.com).

Waste-activated sludge was filtered and the formed filter cake studied. It was shown that average specific filter-cake resistance increases during filtration. A stress–relaxation experiment was performed and the two relaxation times found were of the same order of magnitude as the duration of the filtration stage. It was therefore concluded that the local solid volume fraction of sludge filter cakes changes not only with effective pressure but also with time. In contrast, it is usually assumed in filtration modeling that solid volume fraction is a unique function of effective pressure. A new filtration model was thus developed by adopting the concept of filter-cake creep and applying it in conventional models. It was shown that the model developed, unlike conventional filtration models, satisfactorily describes the experimental data in the case of waste-activated sludge. Furthermore, the model is capable of being scaled with respect to feed concentration and volume. © 2007 American Institute of Chemical Engineers *AIChE J*, 53: 598–609, 2007

Keywords: activated sludge, creep, filtration, modeling

Introduction

Many industries use filtration for solid–liquid separation in such processes as mineral suspensions, fermentation broths, paper pulps, and sludges. Key objectives of filtration are (1) to produce a high filtrate flux and (2) to develop mathematical filtration models to improve the design and operation of filtration equipment.[1,2]

It is assumed in conventional models that there is a unique relationship between local solid volume fraction and local effective pressure during filtration.[2–6] However, such a unique relationship can be questioned in the case of waste-activated sludge[7–9] and other suspensions containing deformable particles.[10,11] La Heij et al.[7] filtered sewage sludge and observed that solid volume fraction near the filter medium increased with time. The effective pressure remained constant at the filter cake–filter medium interface because the medium resistance was negligible. This result indicates that the solid volume fraction increased at a constant effective pressure—in other words, the filter cake crept. Creep effects have also been observed during the consolidation stage when filtering sludge. It has been shown that roughly 70% of the consolidation is secondary consolidation[9]; that is, 70% of the compression arises from creep deformation.

Filter-cake creep is also important when the filtration process is rate limited by drainage of the liquid, given that the local specific filter-cake resistance is a function of solid volume fraction. However, only a few filtration models found in the literature actually incorporate the concept of filter-cake creep.

Shirato et al.[12,13] proposed a linear viscoelastic model—the so-called Terzaghi–Voigt combined model—to simulate filter-cake deformation during the consolidation stage (the last part of the filtration process). Consolidation is divided into two stages: *primary consolidation*, dominated by the dissipation of pore water and the collapse of the overall structure of the filter cake, and *secondary consolidation*, dominated by creep effects. Primary consolidation is modeled as a spring element and secondary consolidation as a Voigt element. Later, La Heij et al.[14] used the Terzaghi–Voigt com-

Correspondence concerning this article should be addressed to K. Keiding at kk@bio.aau.dk.

bined model to model the entire filtration process. The only change made in their approach is that a variable elastic modulus, which increases with solid volume fraction, is used instead of a constant elastic modulus.

Lu et al.[10] found that equilibrium porosity is not attained instantaneously if the filter cake contains deformable particles, such as *Saccharomyces cerevisiae* or Ca-alginate gel particles. In such cases, a viscoelastic model is used to calculate the variation of cake porosity during cake compression.[10]

Kamst et al.[15] partly removed the liquid phase from palm-oil filter cakes and measured the deformation of the filter cake under constant pressure. Their results indicate that palm-oil filter cakes do creep. A nonlinear constitutive equation was suggested, in which the solid volume fraction is a function of both effective pressure and time, and the equation was used to simulate solid volume fraction distribution throughout the thickness of the filter cake.[15] The model has not been used to model the whole filtration process, but only the consolidation stage.

Finally, Sherwood et al.[16] derived a mathematical model to describe filter-cake creep; their computation predicts a rapid initial compaction of the filter cake, whereas the observed compaction is much slower.[16]

This article presents a new approach to this problem, suggesting a simple filtration model that simulates the filtration and consolidation stages for activated sludge and other materials that form creeping filter cakes.

Traditional Cake Filtration Theory

Friction drag on particles

In cake filtration, a solid–liquid mixture is forced toward a filter medium, which is permeable to the liquid but impermeable to the solid particles. Thus, the liquid passes through the filter medium while the solid particles are deposited on it, forming a porous filter cake. The liquid must flow through the filter cake, resulting in a frictional drag between the liquid and the solid particles, a drag that decreases the liquid pressure. A force balance for a one-dimensional filter cake is given in Eq. 1, assuming that gravity forces, wall friction, and inertial forces are all negligible:[17]

$$\frac{F_s}{A} + p_L = P_{app} \tag{1}$$

where F_s (N) is the accumulated frictional drag on the solid particles between x and L (Figure 1), P_{app} (Pa) is the applied pressure, p_L (Pa) is the liquid pressure, and A (m^2) is the cross-sectional area of the filter cake, perpendicular to the direction of liquid flow. Moreover, effective pressure is defined in the following equation:[17]

$$p_s \equiv \frac{F_s}{A} \tag{2}$$

It is assumed that the particles are in point contact and the internal stresses on the particles are transmitted throughout the filter cake.[18] Thus, the effective pressure is the sum of the drag, surface, and body forces divided by the cross-sectional area.[18] The *effective pressure* has also been variously denoted as solid compressive pressure,[19] solid stress,[20] accumulated drag pressure,[21] and particle pressure.[22]

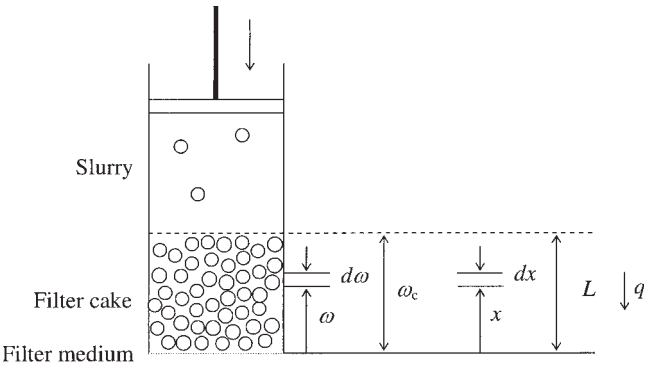

Figure 1. Cake filtration.

It is now possible to substitute Eq. 2 into Eq. 1 and differentiate with respect to distance x, giving the following expression:

$$\left(\frac{dp_L}{dx}\right)_t + \left(\frac{dp_s}{dx}\right)_t = 0 \tag{3}$$

However, material coordinates (ω) are often used instead of space coordinates (x), where ω (kg/m^2) is defined as the mass of dry matter per unit of filter area within distance x of the filter medium, and $d\omega$ is related to dx, as follows:

$$d\omega = \rho_s \phi dx \tag{4a}$$

where ρ_s (kg/m^3) is the solid density and ϕ (dimensionless) is the solid volume fraction (the ratio between the volume of solid material and the total volume). Substituting Eq. 4a into Eq. 3 gives

$$\left(\frac{dp_L}{d\omega}\right)_t + \left(\frac{dp_s}{d\omega}\right)_t = 0 \tag{4b}$$

The liquid pressure gradient in the filter cake can be calculated using the modified Darcy's law:

$$\frac{dp_L}{d\omega} = \mu \alpha q \tag{5}$$

where μ (Pa·s) is the filtrate viscosity, α (m/kg) is the local specific filter-cake resistance, and q (m/s) is the superficial velocity of the liquid relative to the solid particle. Furthermore, substituting Eq. 4b into Eq. 5 yields

$$\frac{dp_s}{d\omega} = -\mu \alpha q \tag{6}$$

Constitutive equations

Local specific filter-cake resistance is a function of solid volume fraction, and expressions have been semitheoretically

derived that describe filter cakes consisting of monodispersed hard spherical particles.[23,24] However, the increase of local specific filter-cake resistance with increasing local solid volume fraction is often underestimated in the case of compressible filter cakes,[25] so alternate constitutive equations have also been used.[17,26]

The effective pressure increases from the top of the filter cake downward to the filter medium as a result of the frictional drag between the liquid and the solid particles.[27–30] Furthermore, compressible filter cakes become compressed when the effective pressure increases, so solid volume fraction is higher near the filter medium than at the top of the cake.[7,30–32] Moreover, solid volume fraction is important when modeling filtrations because the specific filter-cake resistance is a function of solid volume fraction, as described previously. Thus, it is important to know how solid volume fraction depends on effective pressure.

Various constitutive equations describe the equilibrium relationship between solid volume fraction and effective pressure required to compress the filter cake (p_c^{eq}).[17,26] It is usually assumed that the pressure needed to compress the filter cake (p_c) equals p_c^{eq} because slowly changing conditions prevail during filtration processes.[22,33] Moreover, effective pressure increases with time throughout the filtration process; thus $p_s = p_c = p_c^{eq}$. In this case, therefore, effective pressure is a function solely of the solid volume fraction.

Filtrate volume

Two methods can now be used to calculate filtrate volume. In method I it can be calculated from the average specific filter-cake resistance without taking account of the inhomogeneity in the formed filter cake. In method II it can be calculated by numerically modeling the solid volume fraction and the pressure distribution throughout the thickness of the filter cake. It is necessary to determine the average specific filter-cake resistance when using method I and the empirical constants for the constitutive equations, that is, $\alpha(\phi)$ and $p_c^{eq}(\phi)$ when using method II. Only method I will be described for the traditional cake filtration theory.

Average specific filter-cake resistance

The average specific filter-cake resistance α_{av} is defined in the following equation:

$$\alpha_{av} \equiv \frac{p_{s,\omega=0}}{\int_0^{p_{s,\omega=0}} \alpha^{-1} dp_s} \tag{7}$$

where $p_{s,\omega=0}$ (Pa) is the effective pressure at the filter cake–filter medium interface.

The effective pressure at the filter cake–filter medium interface (that is, $p_{s,\omega=0}$) is constant and equal to the applied pressure if the medium resistance is negligible; thus, α_{av} is constant during the filtration stage.

Equation 8 is derived by substituting Eq. 7 into Eq. 6 and integrating the equation. The following boundary condition is used: $p_s = p_{s,\omega=0}$ for $\omega = 0$ and $p_s = 0$ for $\omega = \omega_c$, where ω_c (kg/m^2) is the thickness of the filter cake. Moreover, it is assumed that q is constant throughout the filter cake:

$$q_f = \frac{p_{s,\omega=0}}{\mu \alpha_{av} \omega_c} \tag{8}$$

where q_f (m/s) is the filtrate flux.

The filter-cake thickness can be calculated using Eq. 9, which is a mass balance for the solid particles:

$$\omega_c = \frac{\phi_i}{1-\phi_i}\ \rho_s \left(v_f + \frac{\omega_c}{\rho_s}\ \frac{1-\phi_{cake}}{\phi_{cake}} \right) \tag{9}$$

where ϕ_i is the solid volume fraction of the feed suspension, ϕ_{cake} is the average solid volume fraction of the filter cake, and v_f (m) is filtrate volume per cross-sectional area of the filtration cylinder. The mass of dry matter in the filter cake—the left-hand side of Eq. 9—equals the liquid volume in both the filtrate and filter cake times the mass of dry matter per liquid volume in the feed suspension—the right-hand side of Eq. 9. Equation 9 can be simplified to form

$$\omega_c = \frac{\rho_s}{\frac{1-\phi_i}{\phi_i} - \frac{1-\phi_{cake}}{\phi_{cake}}}\ v_f \tag{10}$$

Substituting Eq. 10 into the inverse function of Eq. 8 gives

$$q_f^{-1} = S^{-1} v_f \tag{11a}$$

where

$$S = \frac{p_{s,\omega=0}}{\mu \alpha_{av} \rho_s} \left(\frac{1-\phi_i}{\phi_i} - \frac{1-\phi_{cake}}{\phi_{cake}} \right) \tag{11b}$$

Furthermore, Eq. 12 can be derived by integrating Eq. 11a with respect to filtration time and setting the lower limit to zero:

$$v_f = (2S)^{1/2} t^{1/2} \tag{12}$$

Thus, filtrate volume increases proportionally with the square root of time, S can be found by fitting Eq. 12 to experimental data, and the average specific filter-cake resistance calculated using Eq. 11b.

Cake Filtration Theory for Filter Cakes that Creep

In the traditional filtration theory, it is assumed that $p_s = p_c = p_c^{eq}$. Nevertheless, $p_c > p_c^{eq}$ for filter cakes that do not instantaneously reach equilibrium when the effective pressure in the filter cake increases. The extra pressure required to compress the filter cake is denoted p_{excess}, such that

$$p_c = p_c^{eq} + p_{excess} \tag{13}$$

Moreover, it will be assumed that p_{excess} increases proportionally with p_c^{eq} and decays exponentially with time; thus

$$\frac{dp_{excess}}{dt} = k\ \frac{dp_c^{eq}}{dt} - \frac{p_{excess}}{\tau} \tag{14}$$

where k is a proportionality factor and τ (s) is a relaxation time.

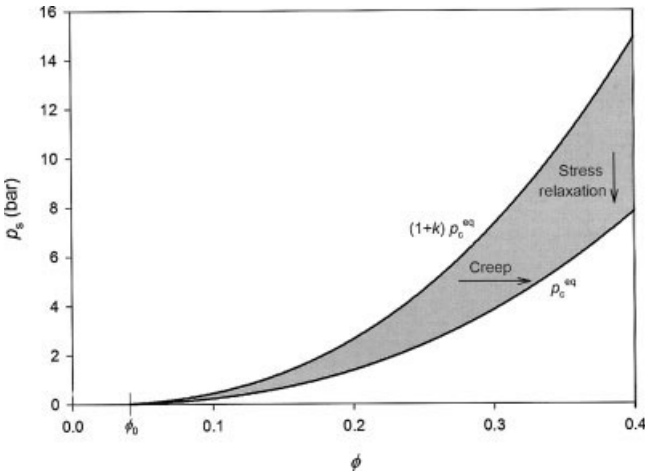

Figure 2. Effective pressure as function of solid volume fraction for filter cakes that creep.

Thus, setting $p_s = p_c$ and combining Eqs. 13 and 14 give

$$p_s^{\min} = p_c^{eq} \tag{15}$$

and

$$p_s^{\max} = (1+k)p_c^{eq} \tag{16}$$

where, at a given solid volume fraction, $p_s^{\min}$ (Pa) is the minimum effective pressure and $p_s^{\max}$ (Pa) is the maximum effective pressure. Thus, p_s is given as a value between p_c^s and $(1+k)p_c^{eq}$, as shown in Figure 2.

Average specific filter-cake resistance (with creep)

Solid volume fraction increases with time if the filter cake creeps during the filtration stage. The average specific filter-cake resistance is therefore not constant and cannot be calculated using either Eq. 11a or Eq. 12. However, Eq. 17, derived by rearranging Eq. 8 and substituting Eq. 10, can be used instead:

$$\alpha_{av}(t) = \frac{p_{L,\omega c}(t)}{\mu q_f(t)\frac{\rho_s}{\frac{1-\phi_i}{\phi_i}-\frac{1-\phi_{cake}}{\phi_{cake}}}v_f(t)} \tag{17}$$

Moreover, Eq. 18 can be fitted to the experimental data if the average specific filter-cake resistance increases from a minimum value, $\alpha_{av}^{\min}$, and asymptotically up to a maximum value, $\alpha_{av}^{\max}$:

$$\alpha_{av}(t) = \alpha_{av}^{\min} + \left(\alpha_{av}^{\max} - \alpha_{av}^{\min}\right)\left(1 - e^{-t/\tau'}\right) \tag{18}$$

where τ' is a time constant. It is then possible to calculate the filtrate volume from Eqs. 11a, 11b, 18, and 19:

$$v_f = \int_0^t q_f dt \tag{19}$$

Note that α_{av} is almost constant at low values of v_f, where the filtration time $\ll$ the relaxation time τ. Thus, the initial value of S can be calculated by fitting Eq. 11a to experimental data obtained during the initial part of the filtration. Moreover, the values determined for S increase linearly with $(1-\phi_i)/\phi_i$ (cf. Eq. 11b), and it is possible to calculate $\alpha_{av}^{\min}$ from the slope of the S vs. $(1-\phi_i)/\phi_i$ relationship using the following equation:

$$\alpha_{av}^{\min} = \frac{p_{L,\omega c}}{\mu \cdot \text{Slope} \cdot \rho_s} \tag{20}$$

Furthermore, ϕ_{cake} can be calculated using the following equation:

$$\frac{1-\phi_i}{\phi_i} \to \frac{1-\phi_{cake}}{\phi_{cake}} \quad \text{for} \quad S \to 0 \tag{21}$$

Thus, $\alpha_{av}^{\min}$ and ϕ_{cake} can be calculated from Eqs. 20 and 21, respectively. The average specific filter-cake resistance can then be calculated from the experimental data using Eqs. 17 and 18 fitted to the result, to determine $\alpha_{av}^{\max}$ and τ'.

Filtration model for filter cakes that creep

The filtrate volume can be calculated for both the filtration and the consolidation stages if the solid volume fraction and pressure distribution throughout the thickness of the filter cake are modeled numerically. This can be done using the modified Darcy's law—that is, Eq. 6, the mass balance for the liquid, and three constitutive equations: Eq. 14, $\alpha(\phi)$, and $p_c^{eq}(\phi)$. The mass balance for the liquid is given as

$$\frac{de}{dt} = \frac{dq}{d\omega} \tag{22}$$

where e is the void ratio defined as

$$e = \frac{1-\phi}{\phi} \tag{23}$$

An equation for $\alpha(\phi)$ can be derived by combining two constitutive equations obtained from Tiller and Leu:[17]

$$\alpha = \alpha_0 \phi^m \tag{24}$$

where α_0 (m/kg) and m are empirical constants. The value of m has been calculated to be 5 ± 2 (standard deviation) by using data from 20 different filtration experiments. These data were obtained from filtrations of attapulgite,[33] $CaCO_3$ with a mean diameter of 3.41 μm and kaolin with a mean diameter of 2.22 μm,[19] Hong Kong kaolin, kaolin, Mierlo biosolid, activated sludge, water treatment residue, carbon iron grade E,[18] $CaCO_3$ with an average particle size of 5 μm and $CiSiO_3$ with an average particle size of 10 μm,[29] a mixture of 66.7% TiO_2 and 33.3% perlite,[17] industrial sludge,[34] and conditioned activated sludge.[14] Moreover, data from six experiments performed on $CaCO_3$ were included.[35]

An often used equation for calculating p_c^{eq} is the following expression:[17,26]

$$p_c^{eq} = p_a\left[\left(\frac{\phi}{\phi_0}\right)^{1/\beta} - 1\right] \tag{25}$$

where β and p_a are empirical constants and ϕ_0 is the solid volume fraction at zero effective pressure.

The empirical constants in the constitutive equation must be known. The empirical constants in Eq. 25 are usually obtained during filtration experiments in which the filter cake is compressed until it stops compressing.[17,36] The effective pressure is assumed to be uniform throughout the filter cake and equal to the applied pressure as well as to p_c^{eq}. Thus, β, p_a, and ϕ_0 can be found by measuring the dry matter content of filter cakes compressed at different applied pressures and fitting Eq. 25 to the measured values. In this study, ϕ_0 is set slightly lower than the calculated ϕ_{cake}, after which β and p_a are calculated by fitting Eq. 25 to the experimental data.

The empirical constants in Eq. 24 can be calculated from α_{av}^{min} and α_{av}^{max}, which are found by fitting Eq. 18 to experimental data, as already described. A function for α_{av}^{min} and α_{av}^{max} can be derived by substituting Eqs. 16 and 15, respectively, into Eqs. 7, 24, and 25 as follows:

$$\alpha_{av}^{min} = \frac{\alpha_0 p_{L,\omega c}(1-m\beta)}{\phi_0^{-m}\{[p_a(1+k)+p_{s,\omega=0}]^{-m\beta}[p_a^{m\beta+1}(1+k)^{m\beta+1}+ p_a^{m\beta}(1+k)^{m\beta}p_{s,\omega=0}] - p_a(1+k)\}} \tag{26}$$

and

$$\alpha_{av}^{max} = \frac{\alpha_0 p_{L,\omega c}(1-m\beta)}{\phi_0^{-m}\left[(p_a+p_{s,\omega=0})^{-m\beta}\left(p_a^{m\beta+1}+p_a^{m\beta}p_{s,\omega=0}\right)-p_a\right]} \tag{27}$$

Equations 26 and 27 give the relationship between the average specific filter-cake resistance and the empirical constants α_0 and m.

Finally, the proportionality factor k and the relaxation time τ can be calculated from stress–relaxation experiments in which the effective pressure is measured at constant solid volume fraction. A filter cake is compressed instantaneously, after which the piston position is kept constant. The effective pressure is equal to the applied pressure if the liquid pressure is zero throughout the filter cake, and p_{excess} is equal to the difference between the applied pressure and p_c^{eq} if the compression is reversible.

Integrating Eq. 14 and setting $p_{excess} = k\Delta p_c^{eq}$ immediately after the deformation step ($t = 0$) give

$$p_{excess}(t) = k\Delta p_c^{eq}\exp\left(-\frac{t}{\tau}\right) \tag{28}$$

where Δp_c^{eq} (Pa) is defined as p_c^{eq} after the deformation, minus p_c^{eq} before the deformation. Furthermore, Eq. 29 is obtained by substituting Eq. 28 into Eq. 13 and setting $p_s = p_c$:

$$p_s = p_c^{eq} + k\Delta p_c^{eq}\exp\left(-\frac{t}{\tau}\right) \tag{29}$$

Thus, the relaxation time τ and proportionality factor k can be calculated by fitting Eq. 29 to data obtained from a stress–relaxation experiment.

A more general expression with more than one relaxation time can be used as well:

$$p_s = p_c^{eq} + \Delta p_c^{eq}\sum_{i=1}^{n} k_i \exp\left(-\frac{t}{\tau_i}\right) \tag{30}$$

where k_i represents proportionality factors and τ_i (s) relaxation times.

In this case, the time constant τ_i, nearest to the duration of the filtration stage, is most relevant when modeling the filtration data. It might also be possible to substitute more than one relaxation time into Eq. 14, but this has been avoided here to keep the numerical model as simple as possible.

Experimental

The filtration equipment was similar to that previously described as a filtration/expression cell with liquid pressure sensor.[37,38] It consisted of a piston, a filtration cylinder with an internal diameter of 50 mm, and a base with a No. 41 Whatman filter paper (Whatman, Maidstone, UK) and a porous plate. The 200-mL cylinder was made from a block of polyacetal (POM), and a V-ring seal of nitrile rubber was fitted onto a stainless steel piston. Pressure was delivered by a horizontal bar mounted between two spindles driven by a step motor, and the applied pressure was measured between the bar and the piston by a load cell (HBM strain Gaussian load cell; Hottinger Baldwin Messtechnik GmbH, Darmstadt, Germany). This setup allowed both constant pressure filtrations and stress relaxation experiments. In constant pressure experiments the step motor made single steps until the applied pressure matched the desired pressure. The applied pressure varied within ± 1 kPa of the set pressure during the experiments. In stress relaxation experiments the step motor made single steps until a given deformation of the filter cake was obtained, after which the piston position was kept constant. The piston position was measured by a rotary encoder and the maximum speed of the piston was measured to 2.33 mm/s. Connection to the liquid pressure transducer (Keller type PR21; Keller AG, Winterthur, Switzerland) was made through the interior of the piston. The applied pressure, the position of the piston, and the liquid pressure at the sample–piston interface were monitored throughout the filtration process, and the filtrate volume per cross-sectional area (v_f) was calculated from the measured piston position.

All experiments were performed using waste-activated sludge colleted from Aalborg East WWTP (Aalborg, Denmark). This plant was designed for carbon removal, nitrification, denitrification, as well as chemical and biological phosphorus removal from domestic wastewater to an amount of 100,000 PE (person equivalent). The sludge age was 20–30 days. The collected samples were thickened for nearly 24 h at 5°C, and then decanted; the conductivity was measured to be 0.7–1.0 mS/cm and the pH to be 7.

The following filtration experiments were performed:

(1) *Experiment I*. Five sludge samples (I.A–I.E) of varying dry matter concentrations were filtered at 100 kPa. Data for the samples are shown in Table 1.

(2) *Experiment II*. A 100-mL sample of 16.4 g/L waste-activated sludge was filtered at 100 kPa, and the applied

Table 1. Data for Experiments I.A to I.E

Sample	Dry Matter Concentration (g/L)	Volume (mL)
I.A	6	180
I.B	19	240
I.C	22	51
I.D	24	140
I.E	28	35

pressure was increased from 100 to 200 kPa when the measured liquid pressure at the sample–piston interface was <20 kPa. The procedure was repeated, that is, the pressure was increased from 200 to 300 kPa when the liquid pressure again was <20 kPa, then from 300 to 400 kPa, and finally from 400 to 500 kPa. It was observed that one or two drops of water were squeezed out of the filter cake after each pressure step.

(3) *Experiment III*. A 200-mL sample of 8.7 g/L waste-activated sludge was filtered and consolidated at 100 kPa for 70 h. The filter cake was then compressed by 0.49 mm for 10 s, after which the piston position was kept constant. The liquid pressure and the applied pressure were measured for the next 25 h. The applied pressure increased abruptly immediately after the compression and was then observed to decline over time. One or two drops of water were squeezed out of the filter cake after the deformation step.

(4) *Experiment IV*. Demineralized water was filtered through one, two, three, four, and eight stacked filter papers at 100 kPa, and the data collected were used to calculate the medium resistance. In addition, filter papers were carefully removed from the filter cakes after sludge filtration. Two experiments were performed in which demineralized water was filtered through one and two stacked used filter papers at 50 kPa. The data collected were used to calculate the medium resistance for the filter papers after the sludge filtration tests.

We checked that the pipe connecting the piston to the liquid pressure transducer was filled with liquid at the end of each experiment. Furthermore, the dry matter content of the sludge filter cakes was calculated by measuring the difference between the wet weight and the dry weight of the filter cake. All filter cakes were dried overnight at 110°C.

Numerical modeling

The filtration process was modeled numerically using the finite-difference method.[39] The filtration cylinder was divided into 50 segments, each containing an equal mass of dry matter. p_c^{eq}, p_{excess}, p_s, and α were calculated for each segment. p_{excess}, p_c^{eq}, and α were calculated by using Eqs. 31, 25, and 24, respectively; p_s was calculated by using Eq. 13 and setting $p_s = p_c$.

$$p_{excess,j+1} = p_{excess,j} + \left(k\frac{p_{c,j+1}^{eq} - p_{c,j}^{eq}}{\Delta t} - \frac{p_{excess,j}}{\tau} \right) \Delta t \quad (31)$$

where the superscript j denotes time, Δt (s) is the time step, and $p_{excess,0}$ was set to zero.

The flux out of the each segment was calculated by using the following expression:

$$q_i = -\frac{1}{\mu\alpha_i}\frac{p_{s,i+1} - p_{s,i}}{\Delta\omega} \quad (32)$$

where $\Delta\omega$ is the dry matter content in one segment per filter medium area. The segments were numbered from the piston (i = 1) to the filter medium (i = 50). The flux through the filter medium, that is q_{50}, was calculated by setting $p_{s,i+1} = 0$ and $\Delta\omega$ to half the dry matter content in one segment divided by the filter media area.

The solid volume fraction were then determined by using

$$\frac{1}{\phi_{i,j+1}} = \frac{1}{\phi_{i,j}} + \frac{(q_{i-1,j} - q_{i,j})\Delta t\rho_s}{\Delta\omega A} \quad (33)$$

and $\phi_{0,j}$ was calculated by setting $q_{i-1,j} = 0$.

This procedure was repeated until the liquid pressure at the segment nearest the piston ($p_{L,50}$) was <1% of the applied pressure (Figure 3).

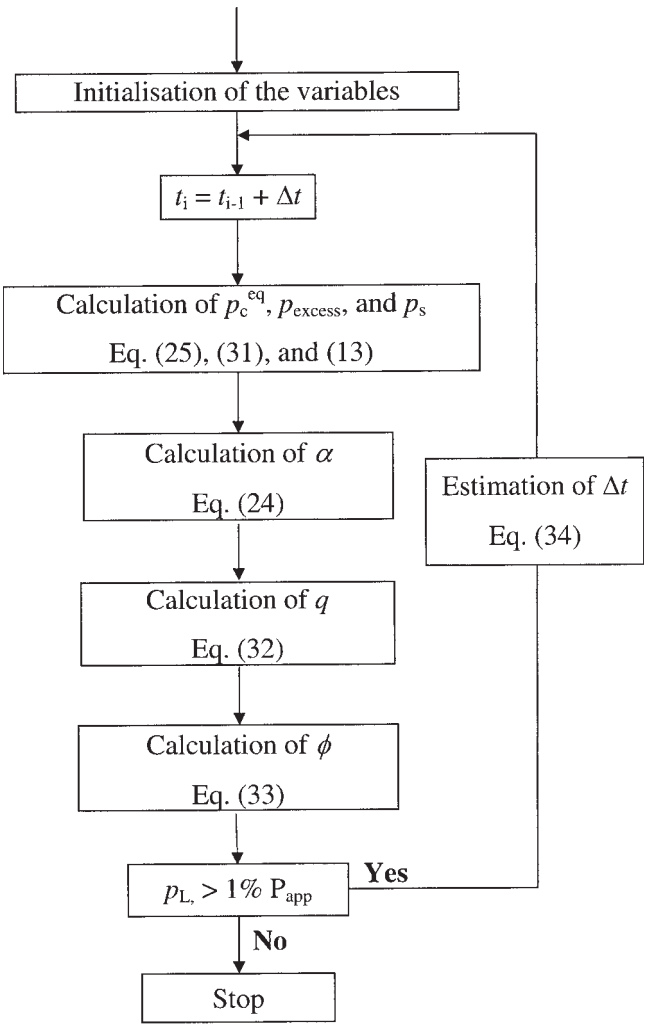

Figure 3. Procedure used to simulate filtrations numerically.

The time step Δt was set to 1×10^{-9} s before the first run and was then calculated after each run using the following equation, which was done to minimize the duration of the simulation and avoid numerical instability:

$$\Delta t = 5 \times 10^{-6} \frac{\Delta\omega}{\rho_s \phi_{\omega=0} q_{\omega=0}} \tag{34}$$

where $\Delta\omega$ (kg/m^2) is the mass of dry matter per square meter in a single segment, and $\phi_\omega = 0$ and $q_\omega = 0$ (m/s) are the solid volume fraction and the superficial liquid velocity, respectively, in the section nearest the filter medium.

The filtration model was fitted to experimental data (from experiment I.A) and τ was adjusted to minimize root mean squared error (RMSE), which was calculated using the following expression:

$$\mathrm{RMSE} = \sqrt{\frac{1}{n}\sum_{i=1}^{n}\left(y_i - y_{est,i}\right)^2} \tag{35}$$

where n is the number of measurements, y_i is the measured value, and $y_{est,i}$ is the estimated value.

The filtration model and the input parameters were afterward used to simulate the filtration data for the four other filtration experiments (experiments I.B–I.E). The RSME was calculated for all experiments.

Results

Medium resistance

The medium resistance was calculated because the medium can influence the course of filtration if the medium resistance is of the same order of magnitude as the total filter-cake resistance. Demineralized water was filtered through both clean and used filter papers (experiment I.E), and it was observed that the filtrate flux remained constant ($\approx$0.01 m/s) for all experiments even when the filter papers were stacked. Thus, the medium resistance was not rate-limiting for the process and it was possible to calculate a maximum value for only the medium resistance. The medium resistance of the clean filter papers was $<1 \times 10^9$ m^{-1} and the resistance of the used filter papers was $<5 \times 10^9$ m^{-1}. In comparison, the filtrate flux for experiment I.A was estimated to be 0.0003 m/s after 8 s and the total resistance was estimated to be 3×10^{10} m^{-1}. Thus, the medium resistance was $<$17% of the total resistance after just 8 s. Given these results, the medium resistance could be safely ignored when studying sludge filter cakes.

Average specific filter-cake resistance (no creep)

A series of experiments was performed to study the filtration properties of sludge and Eq. 12 was fitted to the data using the least-squares method. Figure 4 shows the filtrate volume v_f as a function of filtration time for experiment I.A. S was estimated to be 8.0×10^{-7} m^2/s and α_{av} calculated to be 1.3×10^{13} m/kg. However, the calculated values of v_f were lower than the measured values during the initial part of the filtration stage and higher during the final part. Thus, we concluded that Eq. 12 does not adequately fit the experimental data and thus the data were further analyzed.

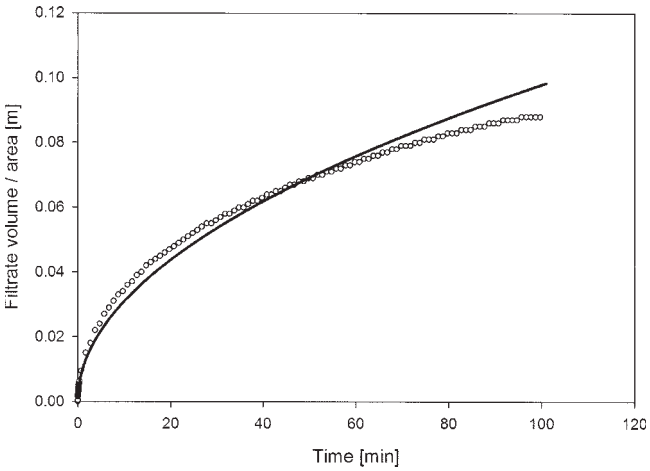

Figure 4. Filtrate volume/area as function of filtration time (experiment I.A).

Equation 12 was fitted to the experimental data using the least-squares method (solid line).

Average specific filter-cake resistance (with creep)

Figure 5a shows the inverse filtrate flux (q_f^{-1}) and liquid pressure as functions of v_f (experiment I.A). Moreover, values for q_f^{-1} were calculated as a function of v_f (solid line). It was observed that the calculated values satisfactorily fitted the experimental data until $v_f = 0.084$ m. Furthermore, it was assumed that the deviation between the calculated and the measured values for $v_f > 0.084$ m was attributed to the fact that the experiment had entered the consolidation stage. The transition point is usually determined as the point where the linearity between q_f^{-1} and v_f ceases.[40] Nevertheless, it was not possible to use this method when filtering waste-activated sludge because q_f^{-1} increased nonlinearly with v_f during the filtration stage. Instead, measurements of the liquid pressure at the sample–piston interface can be used to give an estimate of the filtrate volume at the transition point.[41] The piston touches the filter cake during the consolidation and a gradually increasing part of the piston pressure is transferred directly to the filter cake structure. Thus, the liquid pressure at the sample–piston interface starts to decrease at the transition between filtration and consolidation. The liquid pressure started to decrease rapidly when $v_f \approx 0.087$ m, which corresponds well with the expected filtrate volume at the transition point. A problem with this method was a liquid pressure that was lower than the applied pressure as a result of the friction between the piston and the cylinder. The friction between the piston and the cylinder was therefore calculated by using a modified apparatus where a membrane transducer was placed at the center of the piston in level with the piston head so it was possible to measure the pressure transferred directly from the piston to the sample.[42] The friction between the piston and the cylinder was calculated to roughly 15% and increased during the filtration experiment. The friction in this experiment was determined to 30% of the applied pressure. Furthermore, the liquid pressure decreased in the initial part of the filtration. This might be caused by the transition from dynamic friction to static friction on the friction surfaces between piston and the filtration cylinder.

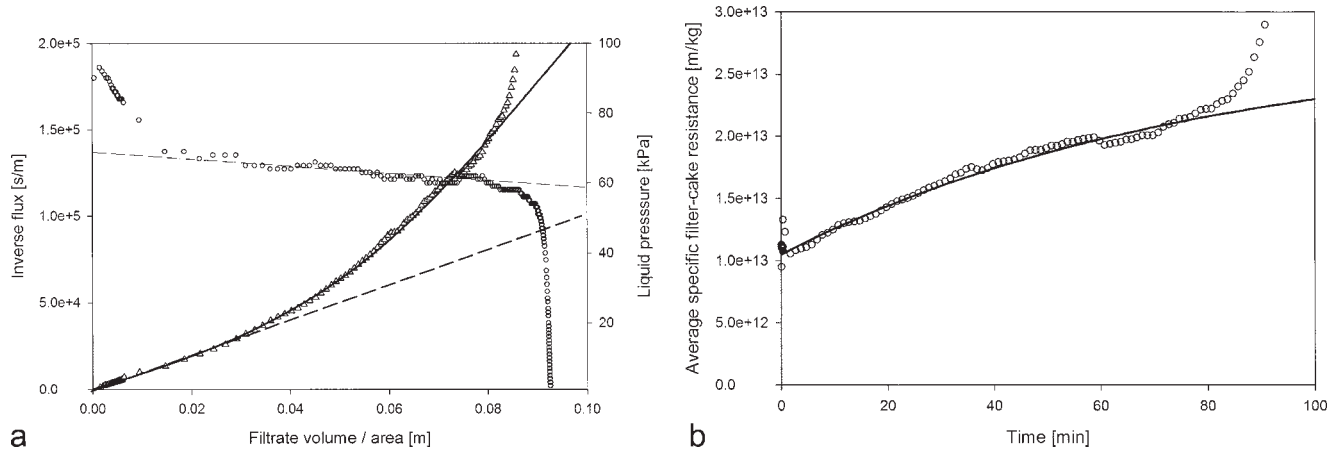

Figure 5. (a) Inverse flux (triangles) and liquid pressure (circles) as function of filtrate volume/area (experiment I.A); the solid line was obtained by calculating the inverse flux from Eqs. 11a, 11b, and 18 and the filtrate volume/area from Eq. 19; the Runge–Kutta Method of Order 4 was used to calculate the filtrate volume/area; the inverse flux increases almost linearly during the initial part of the experiment as shown by the dashed line; (b) the average specific filter-cake resistance as a function of filtration time.

The experimental values (open triangles) were calculated by using Eq. 17 and the solid line was found by using Eq. 18 and setting $\alpha_{av}^{min} = 1.1 \times 10^{13}$ m/kg, $\alpha_{av}^{max} = 2.8 \times 10^{13}$ m/kg, and $\tau' = 1.3$ h.

Figure 5b shows the average specific filter-cake resistance as a function of time. The experimental values (open triangles) were calculated by using Eq. 17 and the solid line was found by using Eq. 18 and setting $\alpha_{av}^{min} = 1.1 \times 10^{13}$ m/kg, $\alpha_{av}^{max} = 2.8 \times 10^{13}$ m/kg, and $\tau' = 1.3$ h. It is evident that the average specific filter-cake resistance increased over the course of the filtration stage.

Figure 6a shows the results for q_f^{-1} as a function of v_f from five experiments (experiments I.A–I.E). The value of q_f^{-1} increased almost linearly with v_f during the initial part of the filtration stage. Straight lines were fitted to data obtained during the initial part of the experiments. Values for S were calculated for each experiment by using Eq. 11a and the values for S were plotted as a function of $\phi_i/(1 - \phi_i)$ in Figure 6b. A linear relationship between S and $\phi_i/(1 - \phi_i)$ was observed ($r^2 = 0.999$). The value of α_{av}^{min} was calculated to be $1.07 \pm 0.02 \times 10^{13}$ m/kg and of ϕ_{cake} to be 0.05 ± 0.01. The remaining constants were found by fitting Eq. 18 to the experimental data obtained during the filtration stage. Equation 18 adequately fitted the experimental data up to the transition point, and we found that $\alpha_{av}^{max} = 2.8 \times 10^{13}$ m/kg and $\tau' = 1.3$ h for experiment I.A (Figure 5b). Thus, according to the proposed creep model the average specific filter-cake resistance more than doubled during the filtration stage. Moreover, the calculated values for the average specific filter-cake resistance were similar to those previously found for waste-activated sludge filtered at 100 kPa.[43]

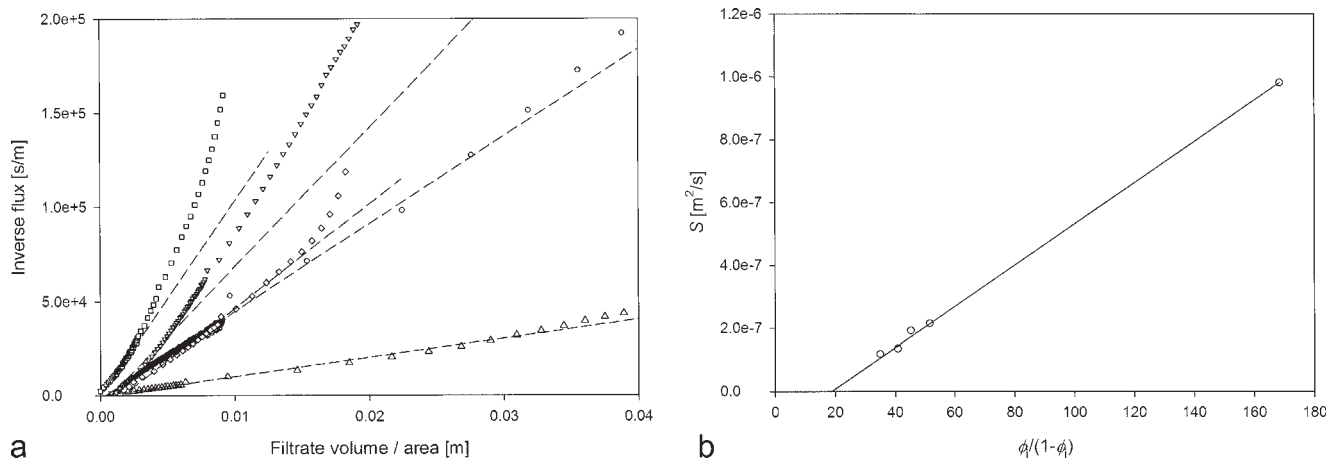

Figure 6. (a) Inverse flux as a function of filtrate volume/area for experiment I.A (triangles), experiment I.B (circles), experiment I.C (diamonds), experiment I.D (inverted triangles), and experiment I.E (squares); straight lines were fitted to data obtained during the initial part of the experiments and the slopes (S^{-1}) calculated; (b) S as a function of the solid volume fraction in the feed suspension.

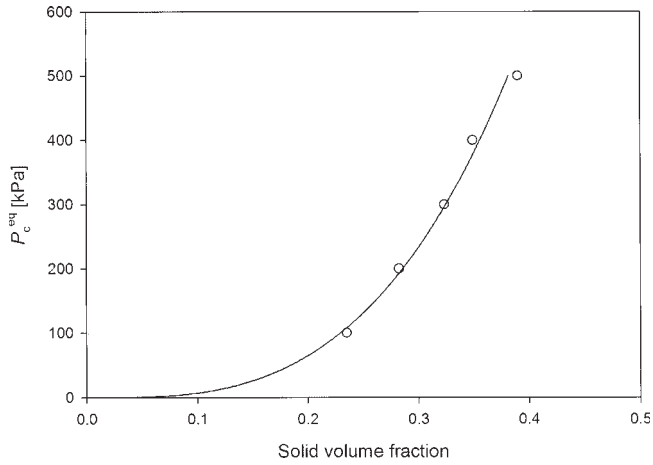

Figure 7. Equilibrium relationship between effective pressure and solid volume fraction.

The experimental data (squares) were obtained from a stepped pressure filtration (Experiment II) and Eq. 25 fitted to the experimental data (solid line).

Filtration model for filter cakes that creep

A filtration model was developed to simulate the filtrate data obtained during both the filtration and consolidation stages. The measured input parameters and simulation results will be described in the following sections.

Figure 7 shows p_c^{eq} vs. ϕ data obtained from the stepped pressure experiment (experiment II). Equation 25 was fitted to the experimental data and the empirical constants β and p_a were calculated. It was not possible to estimate ϕ_0 by fitting the equation to the experimental data because of problems in extrapolating the curve to zero pressure and because of the strong correlation between ϕ_0 and β. Nevertheless, $\phi_0 \leq \phi_{cake} = 0.05$, and the empirical constants shown in Table 2 were found if ϕ_0 was set to 0.04. Furthermore, ϕ_0, β, and p_a were comparable to the empirical constants found for activated sludge.[33]

Figure 8 presents data from the stress–relaxation experiment (experiment III). The liquid pressure at the sample–piston interface was zero after 10 s of compression at elevated pressure and during the stress–relaxation experiment. Thus, the effective pressure was uniform throughout the filter cake, assuming that the friction between the filter cake and the filtration cylinder was negligible. It was assumed that the effective pressure was equal to the applied pressure, that is, the friction loss between the piston and the filtration cylinder was ignored. Equation 30 was fitted to the experimental data setting i = 2, whereby Δp_c^{eq} was calculated to be 130 kPa, k_1 to be 2.3, k_2 to be 0.86, τ_1 to be 0.54 h, and τ_2 to be 7.3 h. The friction loss does not influence the calculated values for Δp_c^{eq}, k_i, and τ_i if the friction loss was constant during the experiment. It was not possible to obtain an acceptable fit to the experimental data if i = 1 (results not shown). Thus, at least two relaxation times were needed to describe the whole course of the stress–relaxation experiment; τ_1 was the relaxation time closest in magnitude to the duration of the filtration stage (experiments I.A–I.E) and was therefore used in the filtration model, whereby τ = 0.54 h and k = 2.3.

Table 2. List of Input Parameters Used in the Filtration Model

Input Parameter	Value
ϕ_0	0.04
β	0.32
p_a	0.40 kPa
k	2.336
τ	0.4 h
α_0	2.5×10^{18} m/kg
m	5

Now, the only remaining unknown input parameters of the filtration model are α_0 and m in Eq. 24. The value of α_0 can be estimated from the minimum average specific filter-cake resistance and Eq. 26, by substituting different values of m into Eq. 26. Some test simulations were performed using values of m ranging from 4 to 6.5 and corresponding values of α_0. The simulation result was not sensitive to the chosen value of m in the studied range. Thus, m was set to 5 and α_0 was calculated to be 2.5×10^{18} m/kg. These values were close to those previously found for activated sludge,[33] where α_0 was calculated to be 3.84×10^{18} m/kg and m was calculated to be 5.4 if the density of the solid material was set to 1000 kg/m^3.

The input parameters were inserted into the filtration model and the filtration data for experiment I.A simulated by setting the pressure to 70 kPa, that is, the applied pressure (100 kPa) minus the estimated friction loss (30 kPa) between the piston and the filtration cylinder. The input parameters are shown in Table 2 and the simulation results are shown in Figures 9a and 9b. The value of τ was changed slightly to improve the results, and RMSE was calculated to be 0.0024 m when the simulated and measured values of v_f were compared. This was <3% of the total sample volume/area. The filtration data obtained from experiments I.B–I.E were also simulated, using the input parameters presented in

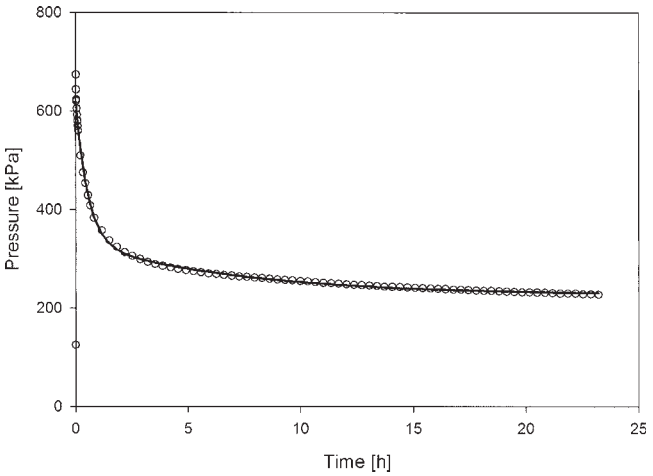

Figure 8. Stress-relaxation experiment (experiment III).

The applied pressure (squares) is shown as a function of time. Equation 30 was fitted to the experimental data setting $i = 2$ (solid line) by using the least-squares method.

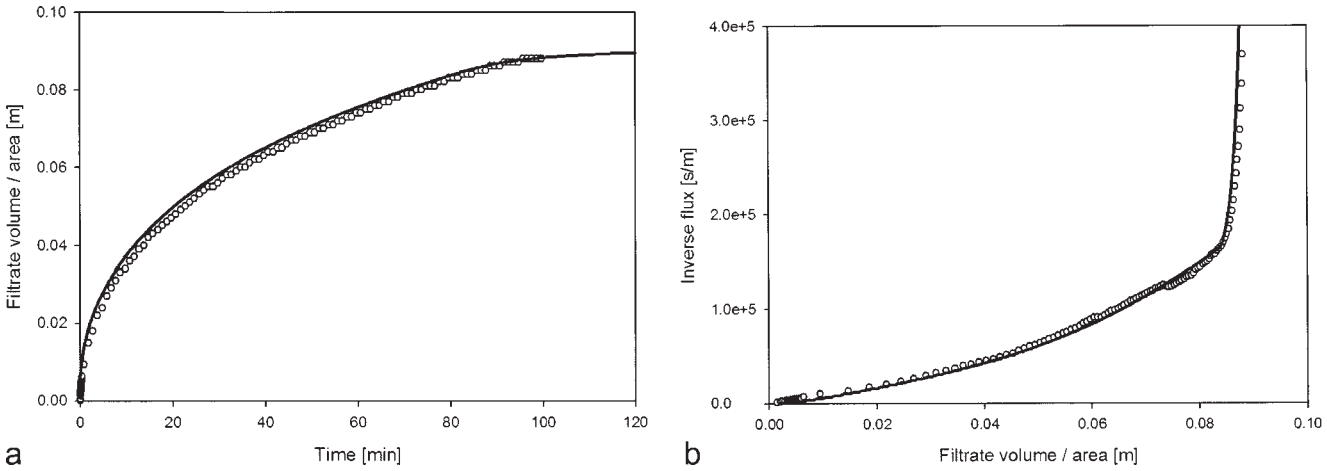

Figure 9. (a) Filtrate volume/area as function of time (experiment I.A). (b) Inverse flux as function of filtrate volume/area (experiment I.A).

Both the experimental data (triangles) and the simulation result (solid line) are shown in the figure.

Table 2. The RMSE ranges from 3 to 6% of the sample volume/area for the other experiments.

Discussion

Filtrate volume increases proportionally with the square root of the filtration time during the filtration stage, if filter-cake thickness increases proportionally with filtrate volume and the average specific filter-cake resistance is constant, as in Eq. 12. Nevertheless, such behavior is not observed when filtering activated sludge (Figure 4). Thus, one or both of the assumptions are not fulfilled, which might be attributable to sedimentation,[44] filter-cake blinding,[45–47] an incorrect determination of the transition between filtration and consolidation,[48] and/or creep.[10,11] There might be other explanations.

Filter-cake thickness does not increase proportionally with filtrate volume if the filter cake is formed by both sedimentation and filtration because the amount of solid deposit per volume of filtrate is high in the initial part of the filtration stage and low afterward. However, sedimentation results in an almost constant value of q_f^{-1} at the end of the filtration stage,[44] which has not been observed when filtering sludge. We thus conclude that sedimentation is not the primary reason for the nonlinear relationship between q_f^{-1} and filtrate volume.

Filter-cake thickness is constant and average specific filter-cake resistance increases when the experiment enters the consolidation stage. Nevertheless, for all experiments a rapid increase of the average specific filter-cake resistance was observed at the end of the experiment (Figure 5b). Moreover, this abrupt increase coincided well with a rapidly decreasing liquid pressure at the sample–piston interface. The only explanation we can find for the observed abrupt increase of the average specific filter-cake resistance and decrease of the liquid pressure is that the experiments entered the consolidation stage. Furthermore, the nonlinear relationship between q_f^{-1} and v_f was observed before this abrupt change of average specific filter-cake resistance and liquid pressure. We therefore conclude that the curvature of the q_f^{-1} vs. v_f plot did not arise from an incorrect determination of the transition between filtration and consolidation.

The average specific filter-cake resistance increases with time if pores in the filter cake are blocked (filter-cake blinding) or if the filter cake creeps. It is difficult to distinguish between blinding and creep solely on the basis of the q_f^{-1} vs. v_f relationship existing in the filtration stage, although filter-cake creep has been observed in the consolidation stage, when blinding effects are negligible.[9] Moreover, a stress–relaxation experiment showed that at least two relaxation times are necessary to fully characterize the relaxation process (Figure 8). The relaxation times determined have the same order of magnitude as the duration of the filtration stage and are similar in magnitude to the relaxation times found for long-chained polymers.[49] Thus, it has been speculated that the relaxation process is a result of the rearrangement of extracellular polymer substances (EPS) in the sludge flocs. However, filtration of other better-defined materials is necessary if we are to obtain a better physicochemical understanding of the relaxation process. Based on these observations, we conclude that the sludge filter cake creeps during the filtration stage, thus causing the average specific filter cake to increase.

Equation 17 has been used to calculate the average specific filter-cake resistance and Eq. 18 is fitted to the obtained result. Equation 18 fits the experimental data well until the filtration process enters the consolidation stage (Figure 5b), and we found that the average specific filter-cake resistance more than doubled during the filtration stage.

A simple new filtration model has been developed by adopting the concept of filter cake creep and applying it in a conventional filtration model (Figures 9a and 9b) by introducing Eqs. 13 and 14. The simulations result in convex curves when q_f^{-1} is plotted as a function of filtrate volume and the model adequately describes the filtration data for experiment I.A (Figure 5a). The same input parameters were used to simulate four other experiments with varying feed concentrations and volumes. The RMSE was $<6\%$ of the sample volume/area in all experiments.

This result was obtained despite the great complexity of waste-activated sludge and the simplicity of the suggested filtration model.

Conclusion

A simple mathematical filtration model has been presented, in which the concept of filter-cake creep is applied in a conventional filtration model. Most of the input parameters for the new filtration model can be determined in the same way as for the conventional filtration model, whereas the remaining input parameters can be found by using a stress–relaxation experiment. Waste-activated sludge has been filtrated and—unlike the conventional filtration models—the new model satisfactorily fit the experimental data.

Acknowledgment

We thank Per Møldrup for critically reading the manuscript.

Notation

A = filter medium area, m^2
e = void ratio
F_s = accumulated frictional drag, N
k = proportionality factor
m = empirical constant
p_a = empirical constant, Pa
P_{app} = applied pressure, Pa
p_c = pressure needed to compress filter cake, Pa
p_c^{eq} = pressure needed to compress filter cake in the equilibrium state, Pa
Δp_c^{eq} = difference between the equilibrium pressure before and after a deformation step, Pa
P_{excess} = difference between the actual pressure needed to compress the filter cake and the pressure needed to compress the filter cake in the equilibrium state, Pa
p_s^{min} = minimum effective pressure at a given solid volume fraction, Pa
p_s^{max} = maximum effective pressure at a given solid volume fraction, Pa
p_L = liquid pressure, Pa
$p_{L,\omega c}$ = liquid pressure at the piston/sample interface, Pa
p_s = effective pressure, Pa
$p_{s,\omega=0}$ = effective pressure at the filter cake/filter medium interface, Pa
q = superficial velocity of the liquid relative to the solid particles, m s^{-1}
q_f = filtrate flux, m s^{-1}
S = defined in Eq. 11b, m^2 s^{-1}
t = filtration time, s
v_f = filtrate volume per filter medium area, m
x = position measured from the filter medium, m

Greek letters

α = local specific filter-cake resistance, m kg^{-1}
α_0 = empirical constant, m kg^{-1}
α_{av} = average specific filter-cake resistance, m kg^{-1}
α_{av}^{min} = minimum average specific filter-cake resistance, m kg^{-1}
α_{av}^{max} = maximum average specific filter-cake resistance, m kg^{-1}
β = empirical constant
ϕ = solid volume fraction
ϕ_{cake} = average solid volume fraction in the filter cake
ϕ_i = solid volume fraction in feed suspension
ϕ^{min} = minimum solid volume fraction at a given effective pressure
ϕ^{max} = maximum solid volume fraction at a given effective pressure
ϕ_0 = solid volume fraction at an effective pressure equal to zero
μ = viscosity of the liquid, Pa·s
ρ_s = density of the solid material, kg m^{-3}
τ = relaxation time, s
τ' = time constant, s
ω = material coordinate measured from the filter medium, kg m^{-2}
ω_c = weight of filter cake per unit area, kg m^{-2}

Literature Cited

1. Landman KA, White LR. Predicting filtration time and maximizing throughput in a pressure filter. *AIChE J*. 1997;43:3147–3160.
2. Sørensen PB, Møldrup P, Hansen JA. Filtration and expression of compressible cakes. *Chem Eng Sci*. 1996;51:967–979.
3. Stamatakis K, Tien C. Cake formation and growth in cake filtration. *Chem Eng Sci*. 1991;46:1917–1933.
4. Wakeman RJ. Numerical-integration of differential-equations describing formation of and flow in compressible filter cakes. *Trans IChemE*. 1978;56:258–265.
5. Keiding K, Rasmussen MR. Osmotic effects in sludge dewatering. *Adv Environ Res*. 2003;7:641–645.
6. Landman KA, Sirakoff C, White LR. Dewatering of flocculated suspensions by pressure filtration. *Phys Fluids A*. 1991;3:1495–1509.
7. LaHeij EJ, Kerkhof PJAM, Kopinga K, Pel L. Determining porosity profiles during filtration and expression of sewage sludge by NMR imaging. *AIChE J*. 1996;42:953–959.
8. Sedin P. On the Determination and Application of Local Filtration Properties. PhD Thesis. Luleå, Sweden: Luleå University of Technology; 2003.
9. Chu CP, Lee DJ. Three stages of consolidation dewatering of sludges. *J Environ Eng ASCE*. 1999;125:959–965.
10. Lu WM, Tung KL, Hung SM, Shiau JS, Hwang KJ. Constant pressure filtration of mono-dispersed deformable particle slurry. *Sep Sci Technol*. 2001;36:2355–2383.
11. Hwang KJ, Lyu SY, Chen FF. The preparation and filtration characteristics of Dextran-MnO_2 gel particles. *Powder Technol*. 2006;161:41–47.
12. Shirato M, Murase T, Tokunaga A, Yamada O. Calculations of consolidation period in expression operations. *J Chem Eng Jpn*. 1974;7:229–231.
13. Shirato M, Murase T, Iwata M, Nakatsuka S. The Terzaghi–Voigt combined model for constant-pressure consolidation of filter cakes and homogeneous semisolid materials. *Chem Eng Sci*. 1986;41:3213–3218.
14. LaHeij EJ, Kerkhof PJAM, Herwijn AJM, Coumans WJ. Fundamental aspects of sludge filtration and expression. *Water Res*. 1996;30:697–703.
15. Kamst GF, Bruinsma OSL, deGraauw J. Solid-phase creep during the expression of palm-oil filter cakes. *AIChE J*. 1997;43:665–672.
16. Sherwood JD, Meeten GH, Farrow CA, Alderman NJ. Concentration profile within nonuniform mudcakes. *J Chem Soc Faraday Trans*. 1991;87:611–618.
17. Tiller FM, Leu WF. Basic data fitting in filtration. *J Chin Inst Chem Eng*. 1980;11:61–70.
18. Tiller FM, Yeh CS. The role of porosity in filtration. IX: Filtration followed by expression. *AIChE J*. 1987;33:1241–1256.
19. Teoh SK, Tan RBH, Tien C. Correlation of C-P cell and filtration test data using a new test cell. *Sep Purif Technol*. 2002;29:131–139.
20. Landman KA, White LR, Eberl M. Pressure filtration of flocculated suspensions. *AIChE J*. 1995;41:1687–1700.
21. Theliander H, Fathi-Najafi M. Simulation of the build-up of a filter cake. *Filtr Sep*. 1996;33:417–421.
22. Landman KA, White LR. Solid/liquid separation of flocculated suspensions. *Adv Colloid Interface Sci*. 1994;51:175–246.
23. Carman PC. Review of literature, confirming validity of Kozeny's theory. *Trans IChemE*. 1937;15:150–166.
24. Happel J. Viscous flow in multiparticle systems—Slow motion of fluids relative to beds of spherical particles. *AIChE J*. 1958;4:197–201.
25. Grace HP. Resistance and compressibility of filter cakes. *Chem Eng Prog*. 1953;49:303–318.
26. Lee DJ, Wang CH. Theories of cake filtration and consolidation and implications to sludge dewatering. *Water Res*. 2000;34:1–20.
27. Massuda M, Bridger K, Harvey M, Tiller FM. Filtration behavior of slurries with varying compressibilities. *Sep Sci Technol*. 1988;23:2159–2174.
28. Tarleton ES, Hadley RC. The application of mechatronic principles in pressure filtration and its impact on filter simulation. *Trans Filtr Soc*. 2003;3:40–47.
29. Fathi-Najafi M, Theliander H. Determination of local filtration properties at constant-pressure. *Sep Technol*. 1995;5:165–178.
30. Johansson C, Theliander H. Measuring concentration and pressure profiles in dead-end filtration. *Trans Filtr Soc*. 2003;3:114–120.

31. Meeten GH. A dissection method for analyzing filter cakes. *Chem Eng Sci*. 1993;48:2391–2398.
32. Tarleton ES. The use of electrode probes in determinations of filter cake formation and batch filter scale-up. *Miner Eng*. 1999;12:1263–1274.
33. Tiller FM, Kwon JH. Role of porosity in filtration. XIII: Behavior of highly compactible cakes. *AIChE J*. 1998;44:2159–2167.
34. Gustavsson K, Oppelstrup J. Consolidation of concentrated suspensions—Numerical simulations using a two-phase fluid model. *Comput Vis Sci*. 2000;3:39–45.
35. Teoh SK, Tan RBH, He D, Tien C. A multifunction test cell for cake filtration studies. *Trans Filtr Soc*. 2001;1:81–90.
36. Usher SP, De Kretser RG, Scales PJ. Validation of a new filtration technique for dewaterability characterization. *AIChE J*. 2001;47:1561–1570.
37. Novak JT, Agerbaek ML, Sorensen BL, Hansen JA. Conditioning, filtering, and expressing waste activated sludge. *J Environ Eng ASCE*. 1999;125:816–824.
38. Andersen NPR. Investigation of Relations between Fundamental Solid/Liquid Suspension Properties and Dewatering Characterisation Parameters. PhD Thesis. Aalborg, Denmark: Aalborg University; 2003.
39. Mathews JH. Numerical Methods for Mathematics, Science and Engineering. Englewood Cliffs, NJ: Prentice Hall; 1992.
40. Tarleton ES, Wakeman RJ. Software applications in filter control, data acquisition and data analysis. *Filtr Sep*. 1999;36:57–64.
41. Christensen ML, Andersen NPR, Hinge M, Keiding K. Characterisation of the transition between the filtration and consolidation stage from liquid pressure measurements. *Trans Filtr Soc*. 2006;6:71–78.
42. Christensen ML. The Effect of Filter Cake Viscoelasticity on Filtration—A Study of Activated Sludge Filtration. PhD Thesis. Aalborg, Denmark: Aalborg University; 2006.
43. Mikkelsen LH, Keiding K. Physico-chemical characteristics of full scale sewage sludges with implications to dewatering. *Water Res*. 2002;36:2451–2462.
44. Christensen GL, Dick RI. Specific resistance measurements—Non-parabolic data. *J Environ Eng ASCE*. 1985;111:243–257.
45. Notebaert FF, Wilms DA, Vanhaute AA. New deduction with a larger application of specific resistance to filtration of sludges. *Water Res*. 1975;9:667–673.
46. Sørensen PB, Christensen JR, Bruus JH. Effect of small-scale solids migration in filter cakes during filtration of waste-water solids suspensions. *Water Environ Res*. 1995;67:25–32.
47. Tien C, Bai RB, Ramarao BV. Analysis of cake growth in cake filtration: Effect of fine particle retention. *AIChE J*. 1997;43:33–44.
48. Stickland AD, De Kretser RG, Scales PJ. Nontraditional constant pressure filtration behavior. *AIChE J*. 2005;51:2481–2488.
49. Bhattacharya M. Stress relaxation of starch synthetic polymer blends. *J Mater Sci*. 1998;33:4131–4139.

Manuscript received May 3, 2006, and revision received Dec. 15, 2006.